Differential Responses to High-Frequency Electrical Stimulation in Brisk-Transient and Delta Retinal Ganglion Cells

Alex E. Hadjinicolaou, Paul Werginz, Jae-Ik Lee, and Shelley I. Fried, *Member, IEEE.*

***Abstract*— Retinal microprostheses strive to evoke a sense of vision in individuals blinded by outer retinal degenerative diseases, by electrically stimulating the surviving retina. It is widely suspected that a stimulation strategy that can selectively activate different retinal ganglion cell types will improve the quality of evoked phosphenes. Previous efforts towards this goal demonstrated the potential for selective ON and OFF brisk-transient cell activation using high-rate (2000 pulses per second, PPS) stimulation. Here, we build upon this earlier work by testing an additional rate of stimulation and additional cell populations. We find considerable variability in responses both within and across individual cell types, but show that the sensitivity of a ganglion cell to repetitive stimulation is highly correlated to its single-pulse threshold. Consistent with this, we found thresholds for both stimuli to be correlated to soma size, and thus likely mediated by the properties of the axon initial segment. The ultimate efficacy of high-rate stimulation will likely depend on several factors, chief among which are (a) the residual ganglion types, and (b) the stimulation frequency.**

I. Introduction

Over the last few decades, the idea of electrically stimulating retinal ganglion cells (RGCs) to restore sight to those blinded by outer retinal degenerative diseases, such as retinitis pigmentosa and age-related macular degeneration, has received considerable attention. Although much progress has been made over this time (see [1] for review), the level of vision granted to patients by a retinal microprosthesis is still somewhat rudimentary and does not allow for more involved visual tasks (such as facial recognition) that require higher levels of spatiotemporal visual detail. Somewhat surprisingly, higher densities of electrode arrays have not led to corresponding benefits in percept quality [2], [3]. These findings suggest that alternative strategies to generate high-quality vision will be needed. It is likely that the substantial difference between the signals evoked from electrically stimulating the retina and the signals arising from the natural processing of visual information in the healthy retina represents a major limitation. Seeing as there are as many as 38,000 ganglion cells/mm^2 in central retina [4] and that there are at least ten different types of RGC that each encode an input visual scene into a unique spiking pattern [5]–[7], it is easy to appreciate that matching the neuronal activity that arises physiologically is no small task.

One of the most fundamental signaling paradigms used by the healthy retina is that ON- and OFF-center RGCs respond to light stimuli in distinct ways: increments in light excite ON cells while simultaneously suppressing OFF cells (the opposite is true for light decrements). Since ON and OFF cells are not activated simultaneously during physiological signaling, a stimulation strategy that can similarly activate each cell type individually is highly desirable. Previous work in rabbit retina found that brisk-transient (BT), direction-selective, and local edge detector ganglion cells have differing sensitivity to single, brief (≤200 μs phase duration) electrical pulses [8]. Further investigation by the same group found that ON- and OFF-BT cells responded differently to high-rate trains (2,000 pulses per second, PPS) of short-duration pulses, suggesting the possibility that the two cell types could be differentially activated by varying the pulse train amplitude [9].

Although short-duration pulses are thought to activate ganglion cells directly by depolarizing the dense band of sodium channels on the proximal axon [8], [10], [11], the mechanism underlying high-frequency activation is less clear. The goal of the present work is to further explore the relationship between single-pulse and high-rate ganglion cell activation.

II. Methods

A. Retinal Preparation and Electrophysiology

The care and use of animals followed all federal and institutional guidelines and all protocols were approved by the Institutional Animal Care and Use Committees of the Boston VA Healthcare System and/or the Subcommittee of Research Animal Care of the Massachusetts General Hospital. Female New Zealand White rabbits (~2 kg; n=23) were anesthetized and subsequently euthanized, after which the eyes were immediately removed. After coronal hemisection of the eyeball, the vitreous was eliminated and the eye cup was dissected to allow the retina to be flattened and separated from the retinal pigment epithelium. The retina was then mounted, photoreceptor-side down, to a 10 mm square piece of Millipore filter paper, which in turn was mounted with vacuum grease to the recording chamber (~1.0 ml volume). The chamber was mounted onto the fixed stage of an upright microscope (Nikon, FN-1), fitted with a 60× water immersion lens. A small hole in the center of the filter paper allowed light stimuli to be projected from below onto the photoreceptor layer.

*Research supported by VA (RR&D: RX001663), NIH (R01-NS110575099700 and R01-EY023651) and the Austrian Science Fund (J3947). All authors were with the Department of Neurosurgery, Massachusetts General Hospital, Harvard Medical School, Boston, MA 02114 USA at the time of this study.

A. E. Hadjinicolaou is now with the Department of Neurology, Massachusetts General Hospital, Harvard Medical School, Boston, MA 02114 USA (e-mail: ahadjinicolaou@mgh.harvard.edu).

P. Werginz is now with the Institute for Analysis and Scientific Computing, Vienna University of Technology, 1040 Vienna, Austria (e-mail: paul.werginz@tuwien.ac.at).

S. I. Fried is also with the Boston VA Healthcare System, Boston, MA 01230 USA (e-mail: fried.shelley@mgh.harvard.edu).

Patch pipettes, filled with Ames medium (Sigma Aldrich, A1420), were used to obtain cell-attached voltage clamp recordings (7-14 MΩ) of retinal ganglion cells using standard procedures [12]. Two Ag/AgCl wires comprised the electrical return, separated by ~8 mm and positioned ~15 mm away from the targeted cell. Over the course of the experiment, the retinal tissue was continuously perfused at 4 mL min^{-1} with Ames medium at ~34°C, equilibrated with 95% O_2 and 5% CO_2. Data were recorded and low-pass filtered at 2 kHz using an Axopatch 200B amplifier (Molecular Devices, Sunnyvale, CA, USA), and digitized at 100 kHz (PCI-MIO-16E-4, National Instruments, Austin, TX, USA). Data acquisition and visual/electric stimulation were controlled by custom software written in LabVIEW (National Instruments, Austin, TX, USA) and MATLAB (Mathworks, Natick, MA, USA).

B. Cell Stimulation and Classification

Light stimuli were centered on the targeted soma and projected onto the photoreceptor outer segments from below using an LCD projector (InFocus, Portland, OR, USA). Recorded cells were subjected to stationary flashed spots (100-1000 μm diameter, 1 s presentation duration) presented on a grey background. Each stimulus was presented at least three times, with at least one second between consecutive presentations. Cells that generated a rapid burst of spikes in response to either bright or dark spots (but not both) were classified as either ON or OFF respectively [6], [7]. Other cell types, including those with sluggish responses [13] were excluded from further analysis. Cells were further classified as either brisk-transient (BT), or delta (Δ), according to previously established criteria [14].

Electrical stimuli were generated by an external constant current source (STG2004, Multi-Channel Systems, MCS GmbH, Reutlingen, Germany) and delivered through a 10 kΩ platinum-iridium electrode (MicroProbes, Gaithersburg, MD, USA). The exposed electrode area was conical (~125 μm height, ~30 μm base diameter), resulting in a surface area of ~5900 μm^2. Stimulating electrodes were positioned 10 μm above the retinal inner limiting membrane by raising the tip of the electrode with a micromanipulator after touching the ILM surface. An iterative process as per [8] was then used to position the electrode at the site of greatest electrical sensitivity, which was generally located 20-60 μm from the soma along the proximal axon. Curves of efficacy (defined as the proportion of stimulus pulses that evoke at least one action potential) were measured by delivering cathodic-leading biphasic pulses (100 μs phase duration, zero interphase, 4-5 current amplitudes, 1-2 μA increments, 9-12 repeats per train) and fitting a two-parameter logistic function. The stimulus amplitude corresponding to 50% efficacy is defined as the *single-pulse threshold* (SPT). Cells that had robust responses to these stimuli were then subjected to 1 kPPS trains of cathodic-leading biphasic pulses (100 μs phase duration, zero interphase duration) delivered using amplitudes of 5-40 μA for 1 s. At least three trials of each amplitude were collected, with 15-20 s delay between trials.

C. Data Analysis

Recordings were processed offline with custom software developed in MATLAB. The strong electrical artifacts generated by high-rate stimulation were removed by subtraction of a scaled, pre-recorded artifact train, and the resulting waveform was smoothed with a 5-frame sliding average to improve the accuracy of spike time detection. Spike times were defined as the depolarization peak of each spike. All data are presented as the mean ± one standard deviation, unless otherwise specified. Pearson's correlation coefficient (ρ) was used to quantify the strength of linear relationships. Soma diameter was measured by capturing a snapshot of the microscope's view of the targeted cell, circumscribing the soma perimeter with a concave polygon and computing its area (ImageJ), and computing the diameter of a circle of equivalent area.

III. Results

We recorded the responses of 10 ON cells (7 ON-BT, 3 ON-Δ) and 18 OFF cells (9 OFF-Δ, 9 OFF-BT) to visual and electrical stimulation. As with earlier studies that investigated ganglion cell responses to high-rate stimulation, it was possible to extract elicited spikes by removing the electrical artifact within the raw recorded waveform by careful signal processing [9], [15], [16]. Fig 1A shows the spikes extracted from an OFF-Δ cell (bottom trace) in response to a 10 μA, 1 kPPS stimulus (top trace). Fig 1B shows spike raster plots of the same cell in response to high-rate pulse trains, with amplitudes ranging from 5-40 μA (three repeats at each amplitude). The number of elicited spikes increases with stimulus amplitude, but only up to a certain amplitude (in this case, 25 μA); we refer to this amplitude as the *peak response amplitude* (PRA). Further increases in stimulus amplitude beyond the PRA yield successively fewer spikes (Fig 1B, 1C). A plot of the total number of elicited spikes versus stimulus amplitude (Fig 1C) shows this relationship more clearly, highlighting the peak response amplitude.

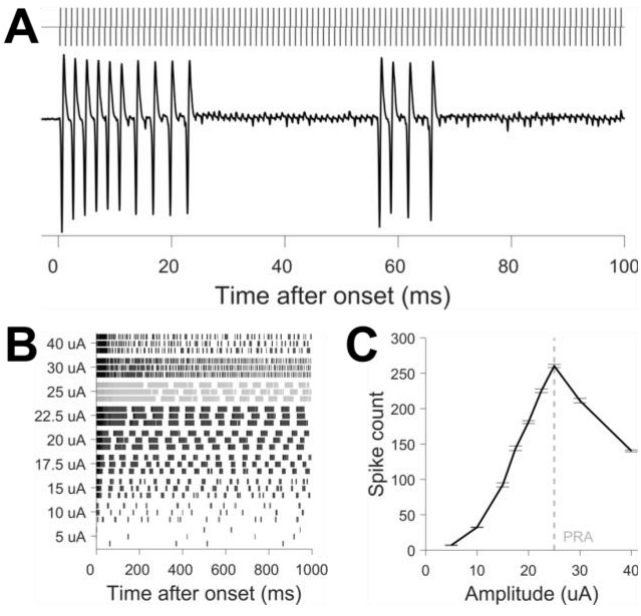

Figure 1. Ganglion cell response to high-frequency pulsatile stimulation. (A) Top: schematic of a 10 μA biphasic pulse train delivered at 1 kPPS. Bottom: recorded response of an OFF-Δ cell to the stimulus, after subtraction of the stimulus artifact. (B) Spike raster plots in response to 1 kPPS stimuli. Each row represents a single trial of the indicated stimulus amplitude. (C) The average number of spikes plotted against stimulus amplitude, with the grey vertical line indicating the peak response amplitude (PRA) at 25 μA. Error bars indicate ±1 standard error.

A. *Responses to High-Rate Stimuli*

In general, all cells tested here exhibited a PRA, i.e. responses initially increased for increasing stimulus levels, but decreased for further increases (Fig. 2). Note that there were two delta cells for which we did not observe a reduction in spike count (one ON and one OFF); it is likely that their PRAs exceed the maximum stimulus amplitude tested here. When we compared the averages across the population, ON-cell PRAs (ON-BT: 20.0±3.8 μA, ON-Δ: 28.3±10.4 μA) were larger than OFF (OFF-BT: 16.4±4.4 μA, OFF-Δ: 23.3±11.8 μA) (Fig. 2B), although these differences did not reach significance ($p>0.05$ for all pairs, Welch's t-test). Note that we excluded the ON-Δ population from all significance testing, owing to its low cell count (n=3).

B. *Relationship between SPT and PRA*

We were somewhat surprised by the level of heterogeneity observed within the high-rate responses of each RGC type and questioned whether there was a relationship between the sensitivity of a ganglion cell to single pulses, and its ability to be repetitively activated at high frequency. We determined the single-pulse threshold for each cell (Fig. 3A) and then plotted this value versus the peak response amplitude for the same cell (Fig. 3B). This revealed a strong linear dependence between the two (Pearson's $\rho=0.83$, $p<0.01$; Fig. 3). Further, the relationship held within each type (ON-BT: $\rho=0.88$, $p<0.01$; OFF-BT: $\rho=0.73$, $p<0.03$; OFF-Δ: $\rho=0.91$, $p<0.01$). This correlation is interesting because it suggests the same factors that mediate threshold to singe pulses also influence the response to high-rate stimulation.

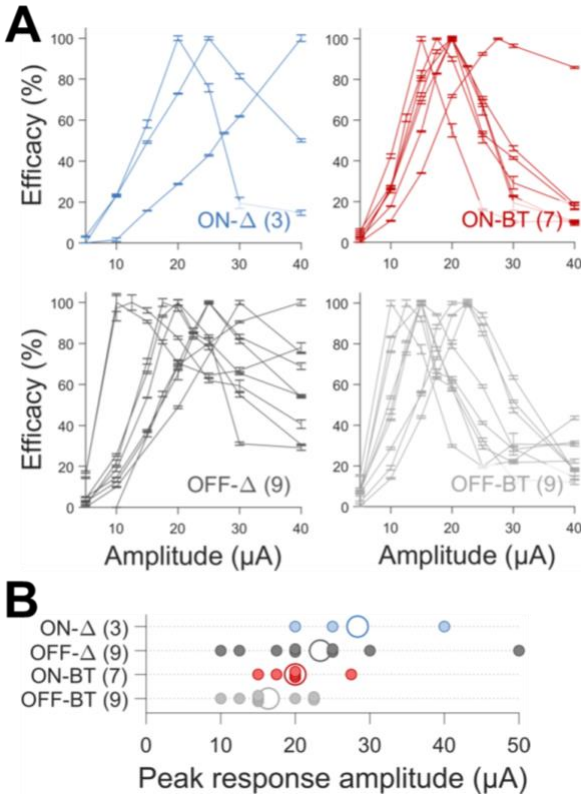

Figure 2. (A) Ganglion cell responses to 1 kPPS stimulation across four cell types. Top row: ON-cells. Bottom row: OFF-cells. Left column: delta cells. Right column: brisk-transient cells. Error bars indicate ±1 standard error. (B) All PRAs, grouped by cell type. Filled markers represent PRAs from a single cell. Larger unfilled markers indicate the mean PRA for each type.

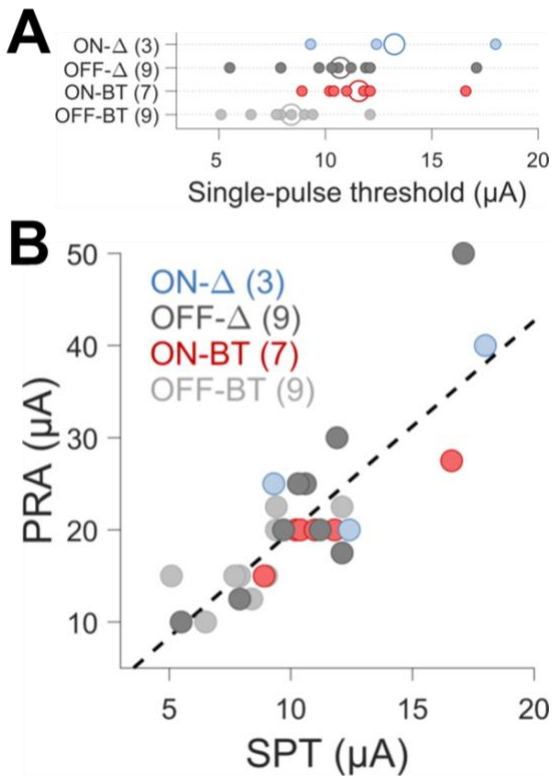

Figure 3. Relationship between single-pulse threshold (SPT) and peak response amplitude (PRA). (A) SPTs of all cells, grouped by cell type. Filled markers represent SPTs from a single cell. Larger unfilled markers indicate the mean SPT for each type. (B) Scatterplot of PRA versus SPT, with linear regression fit traced by the dashed line (adjusted $R^2=0.67$).

ON RGCs tended to have higher SPTs (12.1±3.0 μA) than OFF RGCs (9.5±2.8 μA); differences were statistically significant between the ON- and OFF-BT pair ($p<0.02$) but not the delta pair. SPT thresholds in delta RGCs were higher (11.3±3.5 μA) than those for BT cells (9.8±2.8 μA).

C. *Relationship between SPT and Soma Diameter*

We found that the somata of OFF cells were larger (OFF-BT: 27.7±2.5 μm, OFF-Δ: 24.5±1.9 μm) than those of ON cells (ON-BT: 21.5±2.1 μm, ON-Δ: 20.9±2.7 μm), with significant differences between all non-ON-Δ type pairs ($p<0.02$ for all types; Fig. 4A). Consistent with previous work [17], we found that single-pulse thresholds are moderately correlated with soma size when cell type is not considered ($\rho=-0.50$, $p<0.01$), although this does not hold within cell type ($p>0.1$ for all types).

IV. Discussion

We observed ganglion cell responses to 1 kPPS to be somewhat heterogeneous, across and within cell types in our study, in comparison to those from previous work involving higher-rate stimuli (2 kPPS) [9]. One likely factor that could contribute to this difference is the stimulation rate. Simulations from single-compartment RGC models suggest that the difference between ON and OFF brisk-transient PRA varies as a function of stimulation frequency [18]. A second possible factor is the height of the stimulating electrode, which was positioned closer to the retinal surface in our recordings (5 μm above the inner limiting membrane), versus

that used in the earlier study (10 µm). This difference may have led to qualitative and/or quantitative differences in the recruitment of excitable channels. Finally, the improved methods for cell-type classification used here [14] were not available in previous studies, raising the possibility that there was some contamination of cell types in the previous work.

The relationship between single-pulse threshold and soma diameter is consistent with results from previous studies [8], [17], [19]. Raghuram and colleagues used computer modeling to demonstrate that within a given cell type, larger somata should in fact be associated with larger thresholds [19]. Further, anatomical measurements found that soma size is correlated to the length of the axon initial segment (AIS), the portion of the proximal axon containing dense expressions of sodium channels where spikes are initiated [19], [20]. Longer AISs have been associated with lower activation thresholds [21], [22] and so larger cells are likely to have lower thresholds, providing an explanation for the correlation between soma size and threshold found here.

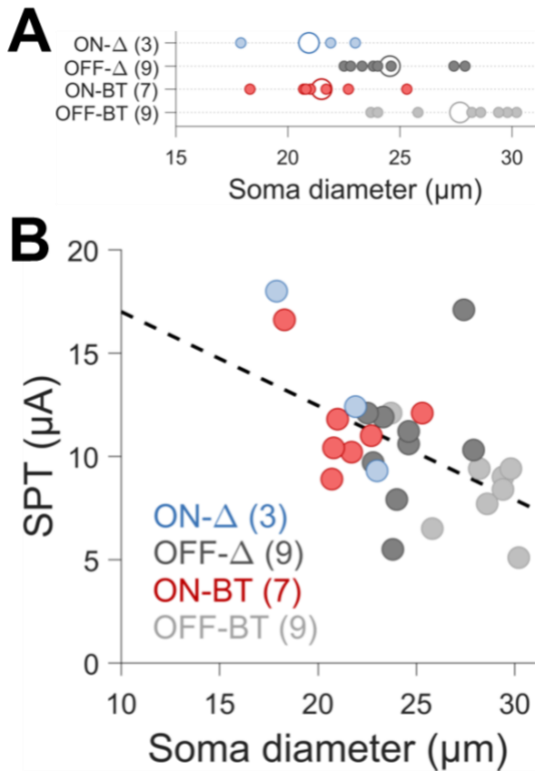

Figure 4. (A) Scatterplots of soma diameter, grouped by ganglion cell type. Filled markers represent values from a single cell. Larger markers indicate the mean value for each type. (B) Scatterplot of single-pulse threshold versus soma diameter, with linear regression fit traced by the dashed line (adjusted R^2=0.22).

References

[1] A. E. Hadjinicolaou, H. Meffin, M. I. Maturana, S. L. Cloherty, and M. R. Ibbotson, "Prosthetic vision: devices, patient outcomes and retinal research: A review of prosthetic vision research," *Clin. Exp. Optom.*, vol. 98, no. 5, pp. 395–410, Sep. 2015, doi: 10.1111/cxo.12342.

[2] E. Zrenner *et al.*, "Subretinal electronic chips allow blind patients to read letters and combine them to words," *Proc. R. Soc. B Biol. Sci.*, vol. 278, no. 1711, pp. 1489–1497, May 2011, doi: 10.1098/rspb.2010.1747.

[3] L. da Cruz *et al.*, "The Argus II epiretinal prosthesis system allows letter and word reading and long-term function in patients with profound vision loss," *Br. J. Ophthalmol.*, vol. 97, pp. 632–636, 2013.

[4] C. A. Curcio and K. A. Allen, "Topography of ganglion cells in human retina," *J. Comp. Neurol.*, vol. 300, no. 1, pp. 5–25, Oct. 1990, doi: 10.1002/cne.903000103.

[5] D. M. Dacey, "Primate retina: cell types, circuits and color opponency," *Prog. Retin. Eye Res.*, vol. 18, no. 6, pp. 737–763, Nov. 1999.

[6] B. Roska and F. Werblin, "Vertical interactions across ten parallel, stacked representations in the mammalian retina," *Nature*, vol. 410, no. 6828, pp. 583–587, 2001.

[7] R. L. Rockhill, F. J. Daly, M. A. MacNeil, S. P. Brown, and R. H. Masland, "The diversity of ganglion cells in a mammalian retina," *J. Neurosci. Off. J. Soc. Neurosci.*, vol. 22, no. 9, pp. 3831–3843, May 2002, doi: 20026369.

[8] S. I. Fried, A. C. W. Lasker, N. J. Desai, D. K. Eddington, and J. F. Rizzo, "Axonal sodium-channel bands shape the response to electric stimulation in retinal ganglion cells," *J. Neurophysiol.*, vol. 101, no. 4, pp. 1972–1987, Apr. 2009, doi: 10.1152/jn.91081.2008.

[9] P. Twyford, C. Cai, and S. Fried, "Differential responses to high-frequency electrical stimulation in ON and OFF retinal ganglion cells," *J. Neural Eng.*, vol. 11, no. 2, p. 025001, Apr. 2014, doi: 10.1088/1741-2560/11/2/025001.

[10] R. J. Greenberg, "Analysis of electrical stimulation of the vertebrate retina: work towards a retinal prosthesis," PhD dissertation, Johns Hopkins University, Baltimore, MD, 1998.

[11] L. G. Nowak and J. Bullier, "Axons, but not cell bodies, are activated by electrical stimulation in cortical gray matter. I. Evidence from chronaxie measurements," *Exp. Brain Res.*, vol. 118, no. 4, pp. 477–488, Feb. 1998.

[12] O. P. Hamill, A. Marty, E. Neher, B. Sakmann, and F. J. Sigworth, "Improved patch-clamp techniques for high-resolution current recording from cells and cell-free membrane patches," *Pflüg. Arch. Eur. J. Physiol.*, vol. 391, no. 2, pp. 85–100, Aug. 1981.

[13] J. H. Caldwell and N. W. Daw, "New properties of rabbit retinal ganglion cells.," *J. Physiol.*, vol. 276, no. 1, pp. 257–276, Mar. 1978, doi: 10.1113/jphysiol.1978.sp012232.

[14] P. Werginz, M. Im, A. E. Hadjinicolaou, and S. I. Fried, "Visual and electric spiking responses of seven types of rabbit retinal ganglion cells," in *2018 40th Annual International Conference of the IEEE Engineering in Medicine and Biology Society (EMBC)*, Honolulu, HI, 2018, pp. 2434–2437, doi: 10.1109/EMBC.2018.8512746.

[15] C. Cai, Q. Ren, N. J. Desai, J. F. Rizzo, and S. I. Fried, "Response variability to high rates of electric stimulation in retinal ganglion cells," *J. Neurophysiol.*, vol. 106, no. 1, pp. 153–162, Jul. 2011, doi: 10.1152/jn.00956.2010.

[16] C. Cai, P. Twyford, and S. Fried, "The response of retinal neurons to high-frequency stimulation," *J. Neural Eng.*, vol. 10, no. 3, p. 036009, Jun. 2013, doi: 10.1088/1741-2560/10/3/036009.

[17] A. K. Cho, A. P. Sampath, and J. D. Weiland, "Physiological response of mouse retinal ganglion cells to electrical stimulation: effect of soma size," *Conf. Proc. Annu. Int. Conf. IEEE Eng. Med. Biol. Soc. IEEE Eng. Med. Biol. Soc. Annu. Conf.*, vol. 2011, pp. 1081–1084, 2011, doi: 10.1109/IEMBS.2011.6090252.

[18] T. Kameneva *et al.*, "Retinal ganglion cells: mechanisms underlying depolarization block and differential responses to high frequency electrical stimulation of ON and OFF cells," *J. Neural Eng.*, vol. 13, no. 1, p. 016017, Feb. 2016, doi: 10.1088/1741-2560/13/1/016017.

[19] V. Raghuram, P. Werginz, and S. I. Fried, "Scaling of the AIS and Somatodendritic Compartments in α S RGCs," *Front. Cell. Neurosci.*, vol. 13, p. 436, Sep. 2019, doi: 10.3389/fncel.2019.00436.

[20] W. Hu, C. Tian, T. Li, M. Yang, H. Hou, and Y. Shu, "Distinct contributions of Na(v)1.6 and Na(v)1.2 in action potential initiation and backpropagation," *Nat. Neurosci.*, vol. 12, no. 8, pp. 996–1002, Aug. 2009, doi: 10.1038/nn.2359.

[21] J. Jeng, S. Tang, A. Molnar, N. J. Desai, and S. I. Fried, "The sodium channel band shapes the response to electric stimulation in retinal ganglion cells," *J. Neural Eng.*, vol. 8, no. 3, p. 036022, Jun. 2011, doi: 10.1088/1741-2560/8/3/036022.

[22] P. Werginz, S. I. Fried, and F. Rattay, "Influence of the sodium channel band on retinal ganglion cell excitation during electric stimulation--a modeling study," *Neuroscience*, vol. 266, pp. 162–177, Apr. 2014, doi: 10.1016/j.neuroscience.2014.01.067.